WATER-WAVE SCATTERING BY SUBMERGED ELASTIC PLATES

by MAHMOOD-UL-HASSAN[†], MICHAEL H. MEYLAN[‡], *and* MALTE A. PETER[§]

(*Department of Mathematics, University of Auckland, Auckland 1142, New Zealand*)

[Received 17 November 2008. Revised 13 March 2009. Accepted 23 March 2009]

Summary

We present a solution to the water-wave interaction with a submerged elastic plate of negligible thickness by the eigenfunction-matching method. The eigenfunction expansion depends on the solution of a special dispersion equation for a submerged elastic plate and this is discussed in detail. We show how the solution can be calculated for the case of normal incidence on a semi-infinite plate in two spatial dimensions and then extend this solution to obliquely incident waves, to a plate of finite length and to a circular finite plate in three dimensions. Numerical calculations showing various properties of the solutions are presented and a near-orthogonality relation for the eigenfunctions is used to derive an energy-balance relation.

1. Introduction

The interaction of linear water waves with submerged plates of small thickness has received considerable research attention, dating back to Dean (**1**) and Ursell (**2**). In the simplest cases, the plate is rigid and either horizontal or vertical, which allows considerable simplifications. If the plate is inclined then the problems become more complicated and they are commonly referred to as barrier problems. Recent work is summarised in Mandal and Chakrabarti (**3**).

The problem of an elastic plate has also been extensively studied, almost exclusively focused on the problem of plates floating on the water surface (since this has applications to scattering by sea ice as well as man-made very large floating structures). Early solutions include Fox and Squire (**4**) for a semi-infinite plate (by eigenfunction matching) and Meylan and Squire (**5**) for a finite plate (using an integral equation). Since then, the elastic plate has been the focus of substantial research and summaries can be found in the review articles Watanabe *et al.* (**6**) and Squire (**7**). However, the problem of a submerged elastic plate seems to have not been considered hitherto, despite the fact that this is the simplest hydroelastic problem with submergence. We present solutions to the two-dimensional problems of a semi-infinite and a finite plate and the three-dimensional problem involving a circular plate.

While the submerged elastic plate problem is somewhat idealised, it is likely that any practical structure that is sufficiently thin to be modelled as of negligible thickness could easily exhibit significant bending. The usefulness of submerged horizontal finite structures as breakwaters or wave barriers has received some research attention, including rigid plates (sometimes referred to as docks)

[†]On leave from Department of Mathematics, COMSATS Institute of Information Technology, Islamabad, Pakistan.
[‡]Corresponding author. (meylan@math.auckland.ac.nz)
[§]Present address: Institute of Mathematics, University of Augsburg, 86135 Augsburg, Germany.

Q. Jl Mech. Appl. Math, Vol. 62. No. 3
Advance Access publication 11 May 2009. doi:10.1093/qjmam/hbp008

(**8**) and membranes (**9**). In the latter work, it is suggested that it might also be useful to investigate an elastic plate rather than a membrane and this is the problem considered here. A major advantage of using horizontal plates (as opposed to structures with vertical extent) is the fact that they allow exchange of water and hardly disturb (horizontal) currents. The use of a stack of horizontal submerged docks as a breakwater is considered in Wang and Shen (**10**). The analogous problem with elastic plates could also be solved by the method presented in this work although we do not follow this direction here. Furthermore, the solution for a submerged elastic plate will be a useful guide to techniques, and to checking numerical code, for more complicated problems in hydroelasticity that involve submergence.

Because the geometry is sufficiently simple, the form of the potential in different regions of the fluid can be found by separation of variables and the solution can then be obtained using matched eigenfunction expansions (**11**). Methods based on eigenfunction matching have been employed in the context of scattering by plates many times (**4**, **8**, **9**, **12**), and it is this method we use in this work. It should be noted that the rapidness of the convergence of the eigenfunction-matching method is somewhat reduced for a submerged plate owing to the singularity of the fluid velocity at the plate tip.

Several problems of interaction of water waves with semi-infinite plates have also been solved by more analytic approaches such as the Wiener–Hopf technique or the residue calculus method (the latter of which is also based on eigenfunction matching), which can lead to more or less explicit solutions and are not affected by the singularity at the plate tip. These include the submerged dock (**13**, **14**, **11**), the elastic plate at the water surface (**15** to **18**) and the submerged porous plate (**19**). While the Wiener–Hopf method can give much more analytical insight into the solution, it requires a structure of semi-infinite extent. The residue calculus method is also restricted to semi-infinite structures but fast convergent representations of the solution to the corresponding finite-structure problem can be obtained in some cases. Solutions for circular plates are unknown for both methods. It is not unlikely that the semi-infinite submerged elastic plate problem can also be solved using a Wiener–Hopf approach or the residue calculus method and that the latter method may also yield a fast convergent representation of the solution for a finite plate.

Nevertheless, we use standard eigenfunction matching in this work because of its generality and its simplicity (both derivation wise and implementation wise). Unlike the other techniques, the eigenfunction-matching method is capable of coping with all three geometries (semi-infinite, finite and circular) in the same way, only requiring very little modifications to move from one to the other. It is noteworthy that this fact seems to have been missed by researchers in the past. For example, it took 10 years to move from the eigenfunction-matching solution for the semi-infinite elastic plate at the surface (**4**) to the corresponding circular plate solution (**12**). The analogous finite plate solution seems to have not been published so far. It is also worth pointing out that the main difficulty of the method, that is, the behaviour and the finding of the roots of the dispersion relation in the plate region (cf. (2.26) below), is also present in the residue calculus method and Wiener–Hopf technique (except for cases where the Cauchy integral method can be employed to avoid the roots in a beneficial way, for example, for the porous plate (**19**)).

The outline of this paper is as follows. We begin in section 2 with the problem of a submerged elastic plate, which we solve by eigenfunction matching. The principal difficulty of this method is to determine the solution of the dispersion equation for the region in which the submerged plate is located, and this is discussed in detail. For most parameter values, the dispersion relation has an infinite number of solutions, which are real and decay, two complex solutions and two purely imaginary solutions that correspond to travelling waves plus the negative of all these solutions (the dispersion equation is even in wave number). The existence of two positive imaginary solutions

means that the submerged elastic plate actually supports two travelling waves with different wavelengths. We show that, once the dispersion equation has been solved, the solution can be calculated straightforwardly, and we present some numerical simulations. In section 3, we modify the solution for the semi-infinite plate to obtain the solution for the finite plate using symmetry and present further numerical solutions. The necessary modification to account for the circular plate are given in section 4. Section 5 is a brief summary, which is followed by three appendices, in which the solution for a rigid plate is given briefly in our notation for reference purposes, a near-orthogonality relation is derived and, finally, an energy-balance relation is determined.

2. Semi-infinite submerged plate

We begin with the problem of a submerged semi-infinite elastic plate. This is the problem we will consider in most detail. The solutions for the finite plate and the circular plate are a relatively straightforward extensions of this solution, as will be seen in sections 3 and 4.

2.1 *Problem formulation*

Cartesian axes are chosen with the mean free surface coinciding with the (x, y)-plane and z measured vertically upwards. The fluid bottom is at $z = -h$. We assume invariance with respect to the y-direction so that the problem is two-dimensional. (We will briefly consider the case of waves incident at an angle in section 2.8.) A submerged elastic plate of negligible thickness is placed along $z = -d$, $0 < x < \infty$, $-\infty < y < \infty$, where $-h < -d < 0$. We assume that all amplitudes are small enough that linear theory applies and we make the usual assumptions that the fluid is inviscid, incompressible and irrotational. We denote the fluid velocity potential by $\overline{\phi}(x, y, z, t)$. It is further assumed that all motion is time harmonic with angular frequency $\omega = \sqrt{\alpha}$ and that the motion is independent of the y-direction. Thus, we can write

$$\overline{\phi}(x, y, z, t) = \mathrm{Re}\{\phi(x, z)\mathrm{e}^{-\mathrm{i}\omega t}\}, \tag{2.1}$$

where Re denotes the real part. The displacement of the plate about $z = -d$ is

$$\overline{W}(x, y, t) = \mathrm{Re}\{W(x)\mathrm{e}^{-\mathrm{i}\omega t}\}. \tag{2.2}$$

The functions $\phi(x, z)$ and $W(x)$ represent the time-independent parts of the complex velocity potential and the plate displacement, respectively.

We consider the equations for the plate–water system in nondimensional form, as the problem is so well known. The derivation and nondimensionalisation are discussed in detail in Meylan (**20**). We nondimensionalise the spatial variables with respect to a length parameter L, the wavelength of the incident wave, for example, the time variables with respect to $\sqrt{g/L}$ and the mass variables with respect to ρL^3, where g is gravitational acceleration and ρ is the density of the water.

The displacement direction is upward positive, so that across $z = -d$, we have

$$\beta\partial_x^4\overline{W}(x, t) + \gamma\,\partial_{tt}\overline{W}(x, t) = f(x, t), \tag{2.3}$$

where β and γ are related to the stiffness and mass of the plate, respectively, and they are given by

$$\beta = \frac{D}{\rho g L^4}, \quad \gamma = \frac{\rho_\mathrm{p} H}{\rho L}, \tag{2.4}$$

where ρ_p is the density of the plate, D is the rigidity constant of the plate and H is the thickness of the plate. The function $f(x,t) = P(x,-d_-,t) - P(x,-d_+,t)$ represents the forcing on the plate and P is the pressure. The linearised Bernoulli equation gives

$$\frac{\partial\overline{\phi}(x,y,z,t)}{\partial t} + \frac{P}{\rho} + gz = 0. \tag{2.5}$$

Using the Bernoulli equation (2.5), we find that $f(x,t) = \partial_t\overline{\phi}(x,-d_+,z,t) - \partial_t\overline{\phi}(x,-d_-,z,t)$. The linearised kinematic boundary condition at the plate is

$$\frac{\partial\overline{W}(x,t)}{\partial t} = \frac{\partial\overline{\phi}(x,y,z,t)}{\partial z}, \quad z = -d. \tag{2.6}$$

Differentiating (2.3) with respect to time and using (2.1), (2.2) and (2.6), we have

$$\beta\partial_x^4\left(\frac{\partial\phi(x,-d)}{\partial z}\right) - \alpha\gamma\,\frac{\partial\phi(x,-d)}{\partial z} = -\alpha[\phi_+(x) - \phi_-(x)], \tag{2.7}$$

where $\phi_\pm(x) = \phi(x,-d_\pm)$ ($+$ and $-$ denote above and below the plate, respectively).

Under the assumptions above, the spatial velocity potential satisfies the Laplace equation

$$\Delta\phi = 0 \tag{2.8}$$

in the fluid with the boundary conditions

$$\frac{\partial\phi}{\partial z} = \alpha\phi \quad \text{on} \quad z = 0, \tag{2.9}$$

$$\frac{\partial\phi}{\partial z} = 0 \quad \text{on} \quad z = -h, \tag{2.10}$$

$$\frac{\partial\phi}{\partial z}\Big|_{z=-d_+} = \frac{\partial\phi}{\partial z}\Big|_{z=-d_-}, \tag{2.11}$$

$$\beta\partial_x^4\left(\frac{\partial\phi}{\partial z}\right) - \alpha\gamma\,\frac{\partial\phi}{\partial z} = -\alpha[\phi_+ - \phi_-] \quad \text{on} \quad z = -d,\ 0 < x < \infty, \tag{2.12}$$

$$|\nabla\phi| = \mathcal{O}(r^{-1/2}) \quad \text{as} \quad r = (x^2 + (z+d)^2)^{1/2} \to 0, \tag{2.13}$$

with two edge conditions. If the plate is clamped, the edge conditions are

$$W(0) = \partial_x W(0) = 0 \tag{2.14}$$

and they read

$$\partial_x^2 W(0) = \partial_x^3 W(0) = 0 \tag{2.15}$$

for a plate whose edge is free to move. Condition (2.13) ensures the correct behaviour of the potential at the plate tip. We also need to apply a radiation condition demanding that the scattered wave field consists of outgoing waves only.

Figure 1 shows the schematic diagram of the problem, along with three regions, which we will use in the solution process.

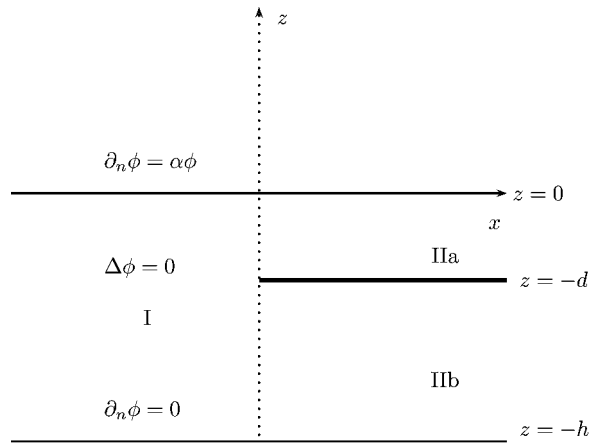

Fig. 1 Schematic setup: submerged elastic plate at $z = -d$, $0 < x < \infty$

2.2 *Region I* $\{-h < z < 0, -\infty < x < 0\}$

The eigenfunction expansion in this region is completely standard and follows from (**11**), and we only summarise the results here. We define k_n, M_n, $\phi_n(z)$, $n = 0, 1, 2, ...$, by

$$\alpha + k_n \tan(k_n h) = 0, \tag{2.16}$$

$$M_n = \frac{h}{2}\left(1 + \frac{\sin(2k_n h)}{2k_n h}\right), \tag{2.17}$$

$$\phi_n(z) = \frac{\cos(k_n(z+h))}{\sqrt{M_n}}, \tag{2.18}$$

where k_n, $n = 1, 2, ...$, are real and positive and k_0 is negative imaginary. The functions $\phi_n(z)$ satisfy the orthonormal relation

$$\int_{-h}^{0} \phi_n(z)\phi_m(z)\,dz = \delta_{mn} \tag{2.19}$$

and they form a complete set over the interval $(-h, 0)$. A general solution for $\phi(x, z)$ in Region I is thus

$$\phi(x, z) = \sum_{n=0}^{\infty} a_n \mathrm{e}^{k_n x}\phi_n(z) + A\mathrm{e}^{-k_0 x}\phi_0(z), \tag{2.20}$$

which satisfies (2.8), (2.9) and (2.10), and $A\mathrm{e}^{-k_0 x}\phi_0(z)$ is the incident wave from $x \to -\infty$ travelling from left to right with amplitude A (in potential).

2.3 *Region II* $\{-h < z < 0, 0 < x < \infty\}$

In Region II, we can separate variables and we find that the potential satisfies

$$\phi(x, z) = \mathrm{e}^{-\kappa x}\psi(z), \tag{2.21}$$

where $\psi(z)$ satisfies

$$\partial_z^2 \psi = -\kappa^2 \psi. \tag{2.22}$$

We can solve for ψ separately in the Regions IIa and IIb and apply the free surface condition and the sea floor condition in each respective domain to obtain

$$\psi(z) = \begin{cases} A(\kappa \cos(\kappa z) + \alpha \sin(\kappa z)), & -d < z < 0, \\ B \cos(\kappa(z+h)), & -h < z < -d. \end{cases} \tag{2.23}$$

Applying the requirement that the normal derivatives above and below the plate match (cf. (2.11)), we obtain

$$(\kappa \sin(\kappa d) + \alpha \cos(\kappa d))A = -\sin(\kappa c)B, \tag{2.24}$$

where $c = h - d$. Therefore, up to multiplication by a constant, ψ can be written as

$$\psi(z) = \begin{cases} -\sin(\kappa c)(\kappa \cos(\kappa z) + \alpha \sin(\kappa z)), & -d < z < 0, \\ (\kappa \sin(\kappa d) + \alpha \cos(\kappa d)) \cos(\kappa(z+h)), & -h < z < -d. \end{cases} \tag{2.25}$$

Applying (2.12) for the Regions IIa or IIb and using (2.24), we get

$$[\beta\kappa^4 - \alpha\gamma\,][\alpha \cos(\kappa d) + \kappa \sin(\kappa d)] \tan(\kappa c) = \alpha \left[\left\{ \frac{\alpha}{\kappa} \sin(\kappa d) - \cos(\kappa d) \right\} \tan(\kappa c) - \frac{\kappa \sin(\kappa d) + \alpha \cos(\kappa d)}{\kappa} \right]. \tag{2.26}$$

This is the dispersion relation for a submerged elastic plate. Before moving on to find an appropriate expansion of the potential in Region II, we discuss the dispersion relation (2.26) in some detail.

2.4 *Properties of the dispersion equation*

The solution of the dispersion equation (2.26) is central to our solution method. First, we note that the equation is even in κ, so that the solutions occur in plus and minus pairs. Moreover, if we have a solution with nonzero imaginary part, its complex conjugate also solves (2.26).

In what follows, we will discuss only the roots that lie in the closed fourth or open first quadrant of the complex plane. The solutions of (2.26) can be divided into three groups for typical plate parameters. We have two negative imaginary solutions, which , which κ_0 and κ_1. There is an infinite number of positive real roots, which correspond to evanescent modes, which we number κ_n, $n \geqslant 2$. We also have two complex roots, which we number κ_{-2} and κ_{-1}. A schematic sketch of the roots is depicted in Fig. 2. Note that for the case when the plate floats on the water surface, the same kinds of roots are found except that there is only one nonnegative imaginary solution.

It is known for the situation where the plate is located at the water surface that the roots may not be distributed in the way presented above. For example, there may be double roots for certain special parameter values (**21**). The determination of the exact behaviour of the roots for all parameters values is a difficult undertaking even for simpler problems, compare (**22**). We also note that, in all cases tested, we find only one complex root in each quadrant. However, we have no proof that this is always the case. In what follows, we consider only parameter values for which the roots are distributed in the way illustrated in Fig. 2. The phenomenon of the complex roots moving onto the

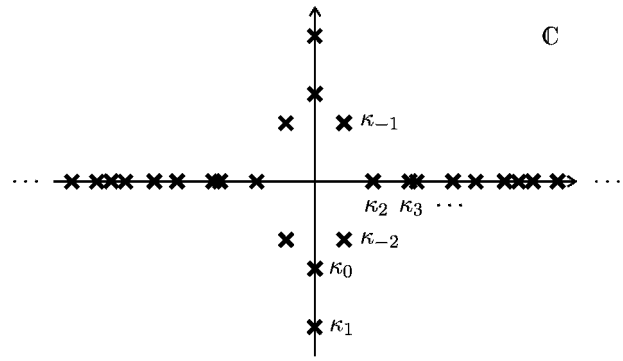

Fig. 2 Schematic sketch of the position of zeros of the dispersion relation (2.26) for the submerged elastic plate

axis is associated with very low fluid density so that the problem approaches that of a plate in a vacuum.

Some well-known situations can be recovered as asymptotic limits of certain parameters. In the limit as $d \to 0$, we recover the dispersion relation for a floating elastic plate (cf. (**4**)). As $\beta, \gamma \to \infty$ (so that the plate becomes stiff and fixed) (2.26) factorises so that we have two dispersion relations

$$\alpha \cos(\kappa_n d) + \kappa_n \sin(\kappa_n d) = 0 \tag{2.27}$$

and

$$\tan(\kappa_n c) = 0. \tag{2.28}$$

Equations (2.27) and (2.28) corresponds to the dispersion relations for a rigid dock (see Appendix A).

For large values of κ_n, (2.26) becomes

$$(\alpha \cos(\kappa_n d) + \kappa_n \sin(\kappa_n d)) \sin(\kappa_n c) = 0. \tag{2.29}$$

and the eigenfunctions ψ_n tend to zero either in the region $-h < z < d$ or in the region $-d < z < 0$.

2.5 *Expansion of the potential in Region II*

We can therefore express the potential in Region II as

$$\phi = \sum_{n=-2}^{\infty} b_n \psi_n(z), \tag{2.30}$$

where

$$\psi_n(z) = \begin{cases} -\sin(\kappa_n c)(\kappa_n \cos(\kappa_n z) + \alpha \sin(\kappa_n z)), & -d < z < 0, \\ (\kappa_n \sin(\kappa_n d) + \alpha \cos(\kappa_n d)) \cos(\kappa_n (z + h)), & -h < z < -d. \end{cases} \tag{2.31}$$

The eigenfunctions are not orthogonal with respect to the standard inner product, but we show in Appendix B that the eigenfunctions ψ_n satisfy a near-orthogonality relation. In what follows we

assume that the eigenfunctions (2.31) form an overcomplete basis so that we can satisfy the boundary conditions at the plate edge. This is analogous to what is done for the elastic plate on the water surface (**4**). In case there is a double root of the dispersion relation (2.26), special eigenfunctions are necessary similar to problems involving porous structures, compare (**23**), for example. We do not consider this case here.

2.6 *Formulation of the system of equations for the semi-infinite elastic plate*

Continuity of the velocity potential (that is, pressure) across $x = 0$ gives

$$A\phi_0(z) + \sum_{n=0}^{\infty} a_n \phi_n(z) = \sum_{n=-2}^{\infty} b_n \psi_n(z). \tag{2.32}$$

Taking the inner product with $\phi_m(z)$ and using (2.19) and (2.31), (2.32) becomes

$$a_m = -A\delta_{m0} + \sum_{n=-2}^{\infty} b_n M_{mn}, \tag{2.33}$$

where

$$M_{mn} = \int_{-h}^{0} \phi_m(z)\psi_n(z)\,dz = -\sin(\kappa_n c)\,p_{mn} + (\kappa_n \sin(\kappa_n d) + \alpha\cos(\kappa_n d))q_{mn} \tag{2.34}$$

and where

$$\begin{aligned} p_{mn} &= \int_{-d}^{0} \{\kappa_n \cos(\kappa_n z) + \alpha \sin(\kappa_n z)\}\phi_m(z)\,dz \\ &= \frac{k_m \sin(ck_m)(\kappa_n \cos(\kappa_n d) - \alpha \sin(\kappa_n d)) + \kappa_n \cos(ck_m)(\alpha \cos(\kappa_n d) + \kappa_n \sin(\kappa_n d))}{(\kappa_n^2 - k_m^2)\sqrt{M_m}} \end{aligned} \tag{2.35}$$

and

$$\begin{aligned} q_{mn} &= \int_{-h}^{-d} \cos(\kappa_n(z+h))\psi_m(z)\,dz \\ &= \frac{\kappa_n \sin(c\kappa_n)\cos(ck_m) - k_m \cos(c\kappa_n)\sin(ck_m)}{(\kappa_n^2 - k_m^2)\sqrt{M_m}}. \end{aligned} \tag{2.36}$$

Continuity of velocity across $x = 0$ gives

$$-Ak_0\phi_0(z) + \sum_{n=0}^{\infty} a_n k_n \phi_n(z) = \sum_{n=-2}^{\infty} -b_n \kappa_n \psi_n(z). \tag{2.37}$$

Again, taking the inner product with $\phi_m(z)$ and using (2.19), (2.37) becomes

$$k_m a_m = -\sum_{n=-2}^{\infty} b_n \kappa_n M_{mn} + Ak_0\delta_{m0}. \tag{2.38}$$

We eliminate a_n from (2.33) and (2.38) and obtain

$$\sum_{n=-2}^{\infty} b_n M_{mn}(k_m + \kappa_n) = A(k_m + k_0)\delta_{m0}. \tag{2.39}$$

2.7 *Numerical solution*

We now need to solve the matching equations (2.33) and (2.39) together with the equations for the edge conditions. The key to our method is to use two more modes on the plate side than are used on the open-water side, so that our matching leaves us requiring two extra equations that we get from the edge conditions (**24**, **12**). If we restrict to $N+1$ modes for the water and $N+3$ for the plate, we obtain the following system of equations to be solved

$$\sum_{n=-2}^{N} b_n M_{mn}(k_m + \kappa_n) = (k_m + Ak_0)\delta_{m0}, \tag{2.40}$$

plus either the clamped-edge conditions

$$\sum_{n=-2}^{N} b_n \kappa_n \sin(\kappa_n c)\{\kappa_n \sin(\kappa_n d) + \alpha \cos(\kappa_n d)\} = 0, \tag{2.41}$$

$$\sum_{n=-2}^{N} b_n \kappa_n^2 \sin(\kappa_n c)\{\kappa_n \sin(\kappa_n d) + \alpha \cos(\kappa_n d)\} = 0, \tag{2.42}$$

or the free-edge conditions

$$\sum_{n=-2}^{N} b_n k_n^3 \sin(\kappa_n c)\{\kappa_n \sin(\kappa_n d) + \alpha \cos(\kappa_n d)\} = 0, \tag{2.43}$$

$$\sum_{n=-2}^{N} b_n k_n^4 \sin(\kappa_n c)\{\kappa_n \sin(\kappa_n d) + \alpha \cos(\kappa_n d)\} = 0. \tag{2.44}$$

Once the b_n are determined, the a_n can be found using (2.33).

2.8 *Obliquely incident waves*

It is relatively simple to include waves incident at an angle. Let us assume that the incident waves are travelling at an angle θ from the normal direction (so that $\theta = 0$ is head-on incidence, which is the case we have been considering so far). This means that we have a wave number $k_y = k_0 \sin\theta$ in the y-direction. When we separate variables, we find the same equations in the vertical direction, so that the wave number in the x-direction is modified and given by $\hat{k}_n$ and $\hat{\kappa}_n$ in the open water and submerged plate region, respectively, where

$$\hat{k}_n = \sqrt{k_n^2 - k_y^2} \tag{2.45}$$

and

$$\hat{\kappa}_n = \sqrt{\kappa_n^2 - k_y^2}, \tag{2.46}$$

where we take the root with positive real part or, in the case when it is purely imaginary, the root with negative imaginary part. Note that for sufficiently large imaginary k_y, the roots $\hat{\kappa}_n$ may be real for $n = 0$ or 1 (values of n for which κ_n is imaginary). This corresponds to the case when there is

only one or no propagating wave in the plate region. The expansion of the potential is then given by

$$\hat{\phi} = \begin{cases} \sum_{n=0}^{N} a_n \mathrm{e}^{\hat{k}_n x} \phi_n(z) + \mathrm{e}^{-\hat{k}_0 x} \phi_0(z), & x < 0, \\ \sum_{n=-2}^{N} b_n^s \mathrm{e}^{\hat{\kappa}_n x} \psi_n(z), & 0 < x. \end{cases} \tag{2.47}$$

The equations to be solved are almost identical to those found before and are given by

$$\hat{k}_m a_m = \sum_{n=-2}^{N} b_n \hat{\kappa}_n M_{mn} + \hat{k}_0 \delta_{m0}, \tag{2.48}$$

$$\sum_{n=-2}^{N} b_n M_{mn} \left(\hat{k}_m + \hat{\kappa}_n \right) = (\hat{k}_m + \hat{k}_0) \delta_{m0}, \tag{2.49}$$

plus either the clamped-edge conditions or the free-edge conditions that are slightly different in this case. They read

$$\left(\frac{\partial^3}{\partial x^3} - (2 - \nu) k_y^2 \frac{\partial}{\partial x} \right) W = 0 \tag{2.50}$$

and

$$\left(\frac{\partial^2}{\partial x^2} - \nu k_y^2 \right) W = 0, \tag{2.51}$$

respectively, where ν is Poisson's ratio.

2.9 *Numerical results*

We present some numerical results. We have taken the water depth to be $h = 1 \cdot 5$ and mass of the plate to be $\gamma = 0 \cdot 1$ for all the following figures. Figure 3 illustrates the behaviour of the modulus of the reflection coefficient $R = a_0$ versus frequency for four different stiffnesses ($\beta = 0 \cdot 01$ (dashed curve), $\beta = 1$ (dotted curve), $\beta = 100$ (chained curve) and $\beta = 10000$ (solid curve)) for the semi-infinite clamped plate. The plate depth is $d = 0 \cdot 5$. We compared these solutions with the solution for a rigid semi-infinite plate (bold dotted line) whose solution is discussed in Appendix A. It can be seen that the amount of reflection increases to a maximum and then decreases with increasing frequency. This is because the plate stiffness is negligible for low-frequency waves, while the plate depth is effectively infinite for high-frequency waves. We can also see that the reflection curves get closer to the rigid plate solution as the plate stiffness is increased and as the frequency increases. In all cases, we have checked our solution against the energy balance and have found good agreement.

Figure 4 is identical to Fig. 3, except the edge conditions are free. It can be seen that the reflections in Fig. 4 for different stiffnesses are less than the corresponding reflections for the same stiffnesses in Fig. 3 as expected since the plate is now free to move. Similarly, the curves in Fig. 4 converge to the rigid plate solution more slowly than for the clamped plate case seen in Fig. 3. However, the qualitative behaviour for the clamped and free plates is similar.

Figure 5 shows the effect of changing the plate depth d for the clamped elastic semi-infinite plate. The plate depths used are $d = 0 \cdot 25$ (dashed), $d = 0 \cdot 5$ (dotted) and $d = 0 \cdot 75$ (dash-dotted). The reflection increases as the submerged plate becomes closer to the water surface. Figure 6 shows the

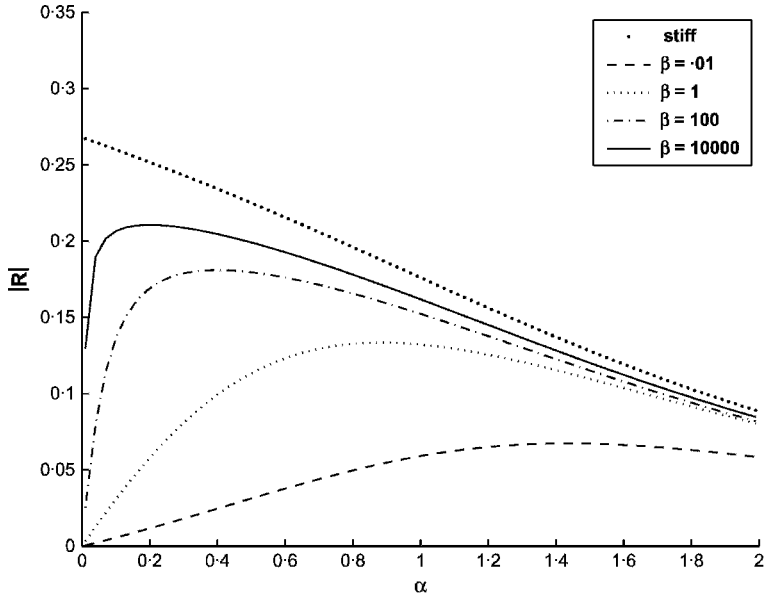

Fig. 3 $|R|$ versus α for the values of β shown for a semi-infinite plate with clamped-edge conditions with $d = 0 \cdot 5$, $h = 1 \cdot 5$ and $\gamma = 0 \cdot 1$

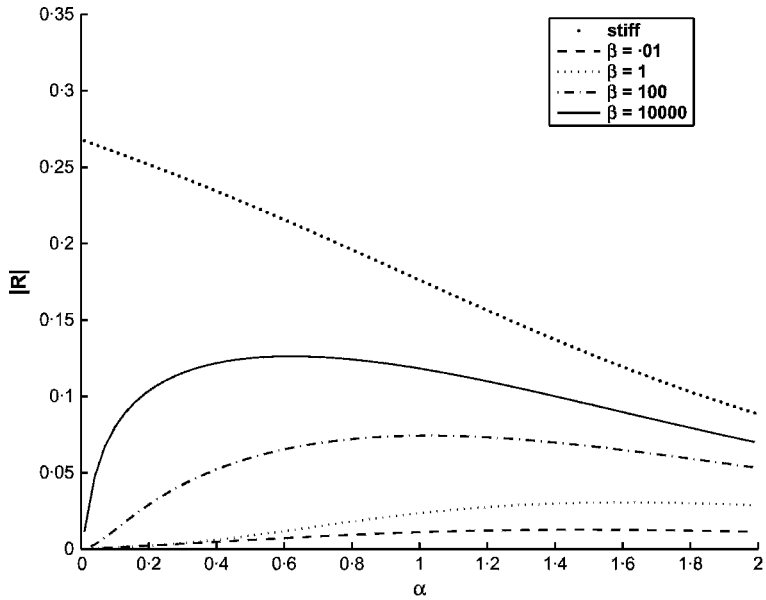

Fig. 4 As in Fig. 3 except free-edge conditions apply for the plate

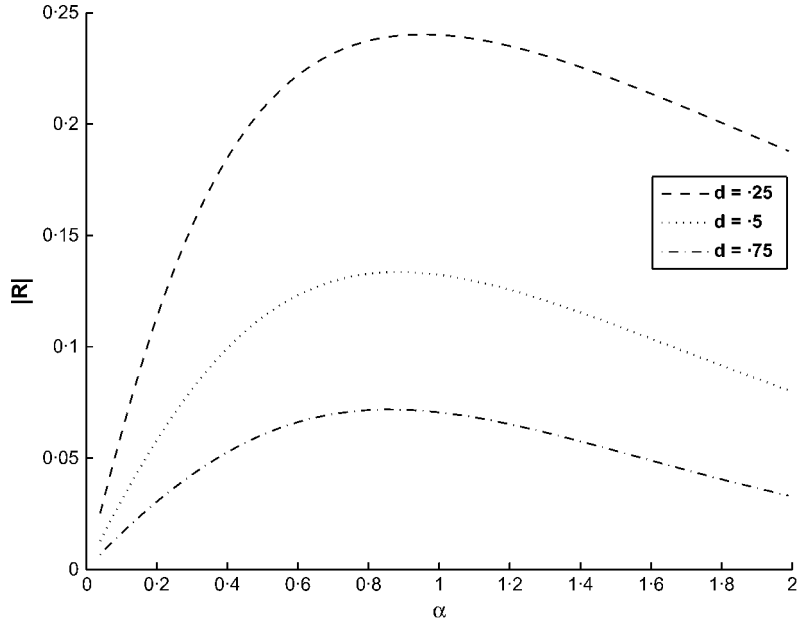

Fig. 5 $|R|$ versus α for the values of d shown for a semi-infinite plate with clamped-edge conditions with $\beta = 1, h = 1 \cdot 5$ and $\gamma = 0 \cdot 1$

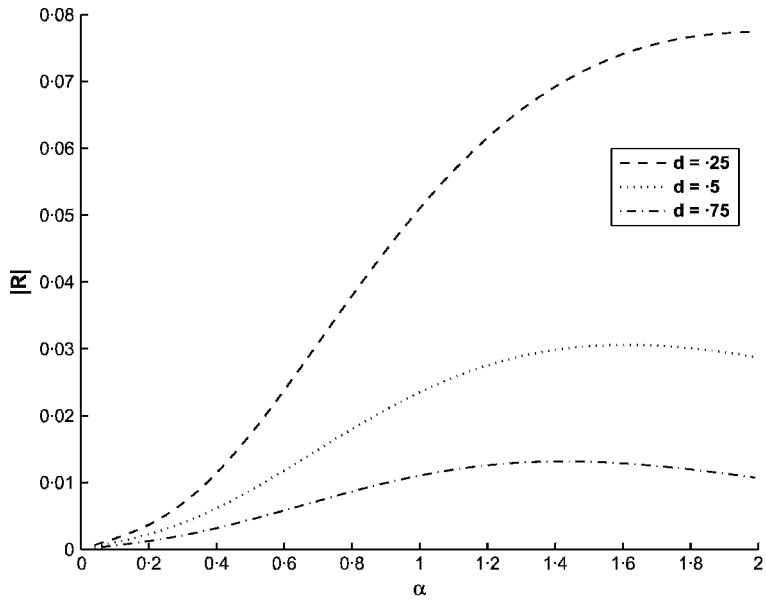

Fig. 6 As in Fig. 5 except free-edge conditions apply for the plate

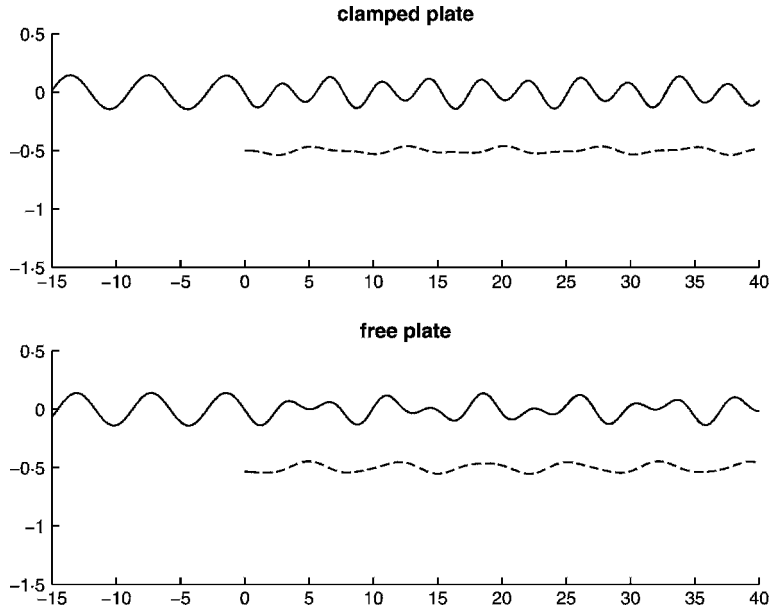

Fig. 7 Surface and plate displacements for a semi-infinite plate with clamped- and free-edge conditions with $\alpha = 1, d = 0 \cdot 5, h = 1 \cdot 5, \beta = 1, \gamma = 0 \cdot 1$ and $A = 0 \cdot 1$. Note that the plate displacement has been drawn with respect to $z = -d$

analogous results to Fig. 5 but for the free-edge conditions. Again, the reflection for the free-edge conditions is less than the reflection for the clamped-edge conditions.

Figure 7 shows the plate and surface displacements for a typical choice of parameters. Note that we have drawn the plate displacement with respect to $z = -d$. The beating effect of the two propagating waves with different wave numbers in the plate region is apparent. Note that we have set the amplitude of the incident wave to be $0 \cdot 1$ to make the figure clearer.

3. Finite elastic submerged plate

In this section, we will consider a finite elastic plate that occupies the line $z = -d$, $-l < x < l$, $-\infty < y < \infty$. The geometry is symmetric about $x = 0$, and so we can decompose the solution into symmetric and antisymmetric solutions about $x = 0$ (**11**). The solution procedure is almost identical for both cases, and the solution method is very similar to that for the semi-infinite submerged plate.

The solution domain is shown in Fig. 8. It is sufficient to consider only the region $x < 0$ since the solution can be extended into the whole fluid region using the symmetry relations $\phi^+(x, z) = \phi^+(-x, z)$ and $\phi^-(x, z) = -\phi^-(-x, z)$, where ϕ^+ and ϕ^- are the symmetric and antisymmetric solutions, which satisfy homogeneous Dirichlet and Neumann conditions at $x = 0$, respectively.

3.1 *Symmetric problem*

We will first consider the symmetric case. Let the velocity potential in this case be given by ϕ^+. We begin with the equations in truncated form, so that we have

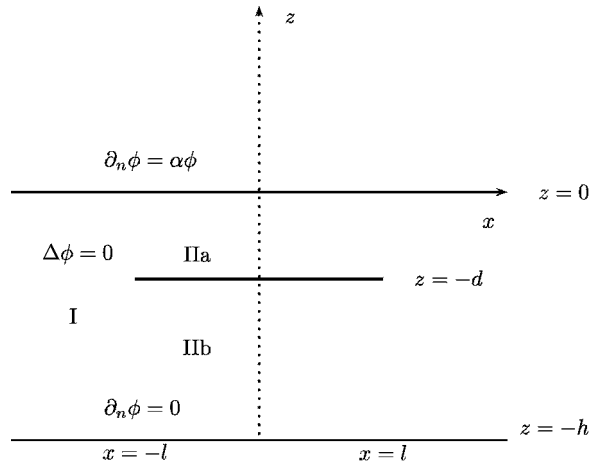

Fig. 8 Submerged finite elastic plate at $z = -d$

$$\phi^+ = \begin{cases} \sum_{n=0}^{N} a_n^+ \mathrm{e}^{k_n(x+l)}\phi_n(z) + A\mathrm{e}^{-k_0(x+l)}\phi_0(z), & x < -l, \\ \sum_{n=-2}^{N} b_n^+ \frac{\cosh(\kappa_n x)}{\cosh(\kappa_n l)}\psi_n(z), & -l < x < 0. \end{cases} \tag{3.1}$$

If we match the potential and its derivative at $x = -l$, we obtain

$$a_m^+ = \sum_{n=-2}^{\infty} b_n^+ M_{mn} + A\delta_{m0} \tag{3.2}$$

and

$$k_m a_m^+ = \sum_{n=-2}^{\infty} b_n^+ \kappa_n \tanh(\kappa_m l) M_{mn} + Ak_0\delta_{m0}. \tag{3.3}$$

We now apply the edge conditions. The clamped-edge conditions (2.14) at $x = -l$ give

$$\sum_{n=-2}^{N} b_n^+ \kappa_n \sin(\kappa_n c)\{\kappa_n \sin(\kappa_n d) + \alpha\cos(\kappa_n d)\} = 0 \tag{3.4}$$

and

$$\sum_{n=-2}^{N} b_n^+ \kappa_n^2 \sin(\kappa_n c)\{\kappa_n \sin(\kappa_n d) + \alpha\cos(\kappa_n d)\}\tanh(\kappa_n l) = 0. \tag{3.5}$$

The free-edge conditions (2.15) at $x = -l$ give

$$\sum_{n=-2}^{\infty} b_n^+ k_n^3 \sin(\kappa_n c)\{\kappa_n \sin(\kappa_n d) + \alpha\cos(\kappa_n d)\} = 0 \tag{3.6}$$

and

$$\sum_{n=-2}^{N} b_n^+ k_n^4 \sin(\kappa_n c)\{\kappa_n \sin(\kappa_n d) + \alpha\cos(\kappa_n d)\}\tanh(\kappa_n l) = 0. \tag{3.7}$$

We solve (3.2) and (3.3) with either the clamped-edge ((3.4) and (3.5)) or the free-edge conditions ((3.6) and (3.7)).

3.2 *Antisymmetric problem*

The antisymmetric solution is very similar to the symmetric problem. We begin with the equations in truncated form. We have

$$\phi^- = \begin{cases} \sum_{n=0}^{N} a_n^- \mathrm{e}^{k_n(x+l)}\phi_n(z) + A\mathrm{e}^{-k_0(x+l)}\phi_0(z), & x < -l, \\ \sum_{n=-2}^{N} b_n^- \frac{\sinh(\kappa_n x)}{\sinh(k_n l)}\psi_n(z), & -l < x < 0. \end{cases} \tag{3.8}$$

Matching the potential and its derivative at $x = -l$, we obtain

$$a_m^- = \sum_{n=-2}^{N} b_n^- M_{mn} + A\delta_{m0} \tag{3.9}$$

and

$$k_m a_m^- = \sum_{n=-2}^{N} b_n^- \kappa_n \coth(\kappa_m l) M_{mn} + Ak_0\delta_{m0}. \tag{3.10}$$

The equations for the clamped-edge conditions are

$$\sum_{n=-2}^{N} b_n^- \kappa_n \sin(\kappa_n c)\{\kappa_n \sin(\kappa_n d) + \alpha\cos(\kappa_n d)\} = 0 \tag{3.11}$$

and

$$\sum_{n=-2}^{N} b_n^- \kappa_n^2 \sin(\kappa_n c)\{\kappa_n \sin(\kappa_n d) + \alpha\cos(\kappa_n d)\}\tanh(\kappa_n l) = 0 \tag{3.12}$$

and the free-edge conditions are

$$\sum_{n=-2}^{\infty} b_n^- k_n^3 \sin(\kappa_n c)\{\kappa_n \sin(\kappa_n d) + \alpha\cos(\kappa_n d)\} = 0 \tag{3.13}$$

and

$$\sum_{n=-2}^{N} b_n^- k_n^4 \sin(\kappa_n c)\{\kappa_n \sin(\kappa_n d) + \alpha\cos(\kappa_n d)\}\tanh(\kappa_n l) = 0. \tag{3.14}$$

As for the symmetric case, we solve (3.9) and (3.10) with either the clamped-edge ((3.11) and (3.12)) or the free-edge conditions ((3.13) and (3.14)). The solution for a wave incident from the left for a finite plate is given by

$$\phi = \frac{1}{2}\left(\phi^+ + \phi^-\right) \tag{3.15}$$

and the reflection and transmission coefficients are given by

$$R = \frac{1}{2}(R^+ + R^-) \tag{3.16}$$

and

$$T = \frac{1}{2}(R^+ - R^-), \tag{3.17}$$

where $R^+ = a_0^+$ and $R^- = a_0^-$.

3.3 *Numerical results*

Figure 9 shows $|R|$ versus α for four different lengths $2l$ of the fixed elastic finite plate, $l = 1$ (dash-dotted), $l = 2$ (dotted) and $l = 5$ (dashed) and the semi-infinite solution (solid). The very complicated behaviour of the finite plate compared with the semi-infinite plate is apparent in this figure. This is due to resonance effects caused by multiple reflections at the water–plate and plate–water boundaries. This is made more complicated by the existence of two travelling waves within the plate region. It can also be seen that, as the plate length is increased, there are more sharp peaks in the response. This is due to the existence of more possible lengths, which give resonances for a longer plate. Figure 10 shows the analogous behaviour of $|R|$ for the free plate. This behaviour here is very similar to that of the clamped plate (Fig. 9) except that there is significantly less reflection, as would be expected for a free plate. We also note the existence of very sharp peaks in the reflection coefficient where the numerical results are close to 1. This is somewhat unusual, and it has never been shown to occur for the case of a finite plate on the water surface.

Figure 11 shows the surface displacements (solid) at $z = 0$ and the plate displacements (dashed) at $z = -d$ for the clamped and free elastic submerged finite plate of length 16 ($l = 8$). This figure also shows the beating effect in the plate region caused by the two travelling modes.

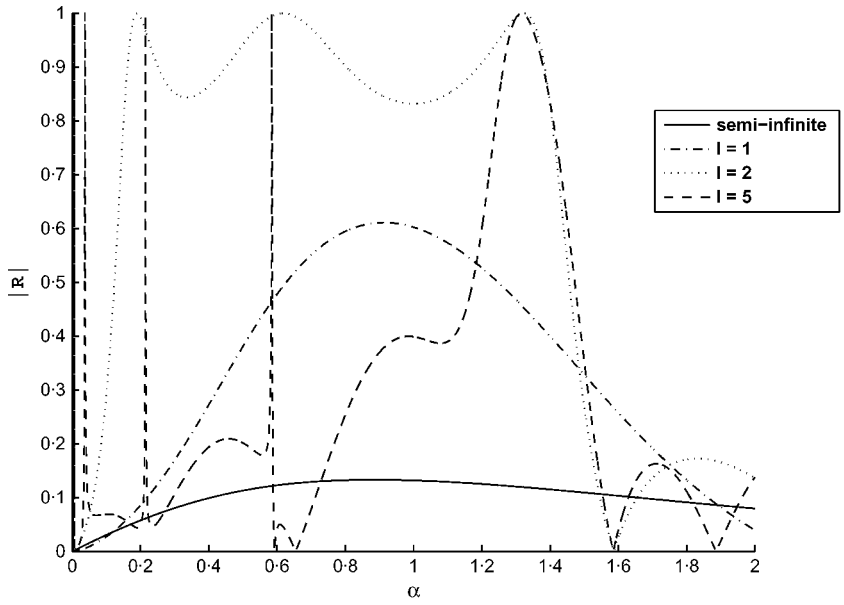

Fig. 9 $|R|$ versus α for the values of l shown for a clamped plate with $d = 0 \cdot 5$, $\beta = 1$, $h = 1 \cdot 5$ and $\gamma = 0 \cdot 1$.

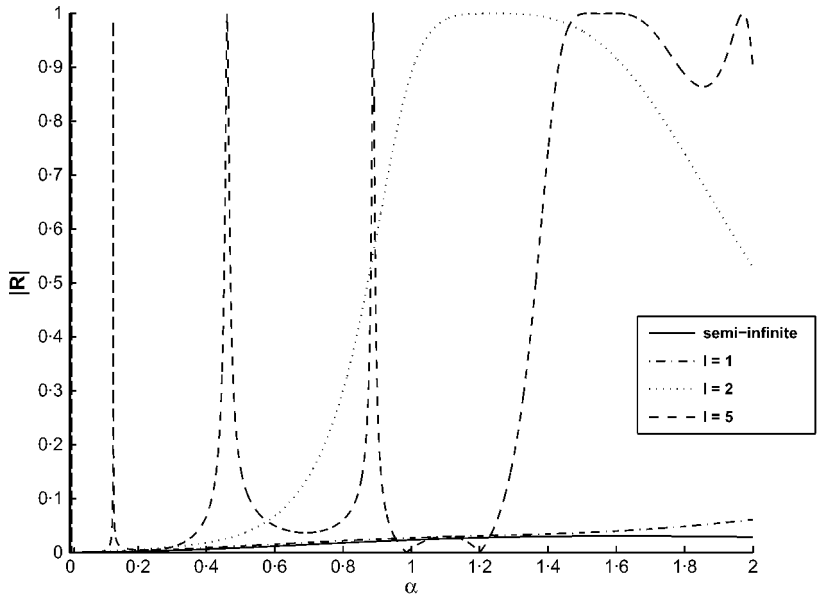

Fig. 10 As in Fig. 9 except free-edge conditions apply for the finite plate

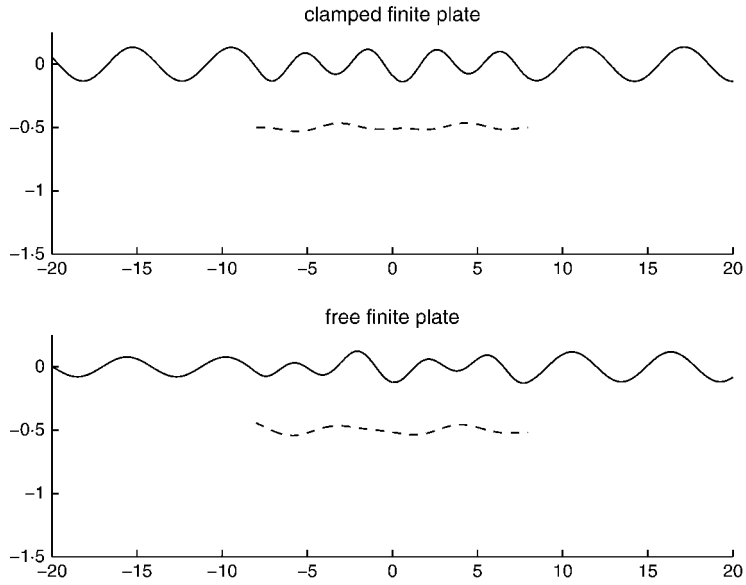

Fig. 11 Surface and plate displacements for the clamped (top) and free (bottom) finite plate. The parameters are chosen as $\alpha = 1, d = 0 \cdot 5, h = 1 \cdot 5, \beta = 1, \gamma = 0 \cdot 1, A = 0 \cdot 1$ and $l = 8$

4. Circular submerged plate

As the vertical eigenfunctions ψ_n are known, the problem of water-wave scattering by a circular submerged elastic plate can also easily be solved. We only give a brief outline here and note that the derivation for the elastic plate at the surface is given in Peter *et al.* (**12**). The derivation of the system of equations for a submerged plate is almost identical to the one in Peter *et al.* (**12**) except that the more complicated vertical eigenfunctions ψ_n need to be used. It is also noteworthy that it is unknown how the problem with circular symmetry can be solved using the Wiener–Hopf technique.

We use a cylindrical coordinate system (r, θ, z) assumed to have its origin at the water surface above the centre of the circular plate with radius a. A sketch of the setup is given in Fig. 12. The plate equation in terms of the three-dimensional velocity potential reads

$$(\beta \triangle^2 - \alpha^2 \gamma) \frac{\partial \phi}{\partial z} = -\alpha^2 [\phi_+(r) - \phi_-(r)] \quad \text{on } z = -d, \ r < a, \tag{4.1}$$

where

$$\triangle = \frac{\partial^2}{\partial r^2} + \frac{1}{r}\frac{\partial}{\partial r} + \frac{1}{r^2}\frac{\partial^2}{\partial \theta^2}. \tag{4.2}$$

The boundary conditions for the plate also change. The vertical force and bending moments must vanish, which (see (**25**)) can be written as

$$[\triangle - \frac{1-\nu}{r}(\frac{\partial}{\partial r} + \frac{1}{r}\frac{\partial^2}{\partial \theta^2})]W = 0 \tag{4.3}$$

and

$$[\frac{\partial}{\partial r}\triangle + \frac{1-\nu}{r^2}(\frac{\partial}{\partial r} - \frac{1}{r})\frac{\partial^2}{\partial \theta^2}]W = 0, \tag{4.4}$$

where $W = \frac{\mathrm{i}}{\sqrt{\alpha}}\phi_z(r, \theta, -d)$ is the time-independent surface displacement and ν is Poisson's ratio.

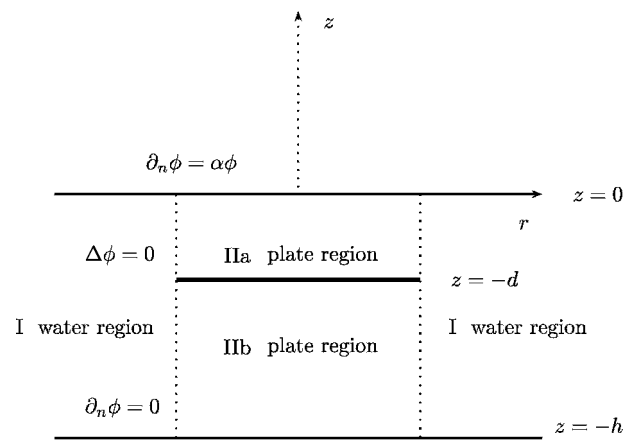

Fig. 12 Submerged circular elastic plate of radius a at $z = -d$

4.1 *Solution method*

Separating variables exploiting the circular symmetry, we can write the potentials as

$$\phi(r,\theta,z) = Z(z)\sum_{s=-\infty}^{\infty} R_s(r)\mathrm{e}^{\mathrm{i}s\theta}, \tag{4.5}$$

where the vertical eigenfunctions $Z(z)$ are given by ϕ_n and ψ_n for $r > a$ and $r < a$, respectively. The appropriate radial eigenfunctions are given in terms of the modified Bessel function $K_s(k_n r)$ and $I_s(\kappa_n r)$ so that

$$\phi(r,\theta,z) = \sum_{s=-\infty}^{\infty}\sum_{n=0}^{\infty} a_{ns}K_s(k_n r)\mathrm{e}^{\mathrm{i}s\theta}\phi_n(z) + \phi^{\mathrm{I}}, \quad r > a, \tag{4.6}$$

$$\phi(r,\theta,z) = \sum_{s=-\infty}^{\infty}\sum_{n=0}^{\infty} b_{ns}I_s(\kappa_n r)\mathrm{e}^{\mathrm{i}s\theta}\psi_n(z), \quad r < a, \tag{4.7}$$

where

$$\phi^{\mathrm{I}} = A\sum_{s=-\infty}^{\infty}(-1)^s I_s(k_0 r)\phi_0(z)\mathrm{e}^{\mathrm{i}s\theta} \tag{4.8}$$

is the incident potential wave of amplitude A in potential travelling in the positive x-direction. Thus, the potential in the open water and plate region are entirely determined by the coefficients a_{ns} and b_{ns}, respectively.

4.2 *Formulation of the infinite dimensional system of equations*

We equate the potential and its derivative at $r = a$ for each s and take the inner product by multiplying both equations by $\phi_s(z)$ and integrating from $-h$ to 0 to obtain:

$$AI_s(k_0 a)\delta_{m0} + a_{sm}K_s(k_m a) = \sum_{n=-2}^{\infty} b_{sn}I_s(\kappa_n a)M_{mn} \tag{4.9}$$

$$Ak_0 I_s'(k_0 a)\delta_{m0} + a_{sm}k_m K_s'(k_m a) = \sum_{n=-2}^{\infty} b_{sn}\kappa_n I_s'(\kappa_n a)M_{mn}. \tag{4.10}$$

The edge conditions ((4.3) and (4.4)) can be expressed in terms of the potentials using the fact that

$$\triangle(I_s(\kappa_n r)e^{is\theta}) = \kappa_n^2 I_s(\kappa_n r)e^{is\theta}, \tag{4.11}$$

giving

$$\sum_{n=-2}^{\infty} b_{sn}\left(\kappa_n^2 I_s(\kappa_n a) - \frac{1-\nu}{a}\left(\kappa_n I_s'(\kappa_n a) - \frac{s^2}{a}I_s(\kappa_n a)\right)\right)\partial_z\psi_n(-d) = 0, \tag{4.12}$$

$$\sum_{n=-2}^{\infty} b_{sn}\left(\kappa_n^3 I_s'(\kappa_n a) - s^2\frac{1-\nu}{a^2}\left(\kappa_n I_s'(\kappa_n a) - \frac{1}{a}I_s(\kappa_n a)\right)\right)\partial_z\psi_n(-d) = 0, \tag{4.13}$$

where

$$\partial_z\psi_n(-d) = -\kappa_n\sin(\kappa_n c)(\kappa_n\sin(\kappa_n d) + \alpha\cos(\kappa_n d)). \tag{4.14}$$

This system of equations can be solved numerically by truncation for each angular mode just as in the previous sections.

It is noteworthy that because the solution is automatically expanded in cylindrical eigenfunctions, it is straightforward to use this method to calculate diffraction transfer operators as are required in the use of general multiple-body interaction theories (**26**, **27**).

5. Conclusions

We have presented the solution for a submerged semi-infinite elastic plate of negligible thickness by the eigenfunction-matching method. This can be seen as an extension of the eigenfunction-matching solutions given for the elastic plate on the water surface and for the submerged rigid plate. The solution method depends on the solution of a special dispersion equation, which has a more complicated structure than the dispersion equation for an elastic plate on the water surface. We showed how the solution for a semi-infinite plate can be extended to waves incident at an angle and to the case of a plate of finite length and a circular plate in the three dimensions. Numerical simulations were presented, which show the complicated behaviour of the system, especially for the finite elastic plate.

6. Acknowledgement

This research was supported by Marsden grant UOO308 from the New Zealand government and by the Higher Education Commission of Pakistan.

References

1. W. R. Dean, On the reflection of surface waves by a submerged plane barrier, *Proc. Camb. Philol. Soc.* **41** (1945) 231–238.

2. F. Ursell, The effect of a fixed vertical barrier on surface waves in deep water, *ibid.* **43** (1947) 374–382.

3. B. N. Mandal and A. Chakrabarti, *Water Wave Scattering by Barriers* (WITpress, Southampton 2000).

4. C. Fox and V. A. Squire, On the oblique reflexion and transmission of ocean waves at shore fast sea ice, *Philos. Trans. R. Soc.* A **347** (1994) 185–218.

5. M. H. Meylan and V. A. Squire, The response of ice floes to ocean waves, *J. Geophys. Res.* **99** (1994) 891–900.

6. E. Watanabe, T. Utsunomiya, and C. M. Wang, Hydroelastic analysis of pontoon-type VLFS: a literature survey, *Engng Struct.* **26** (2004) 245–256.

7. V. A. Squire, Of ocean waves and sea-ice revisited, *Cold Regions Sci. Tech.* **49** (2007) 110–133.

8. H.-F. Cheong, N. Jothi Shankar, and S. Nallayarasu, Analysis of submerged platform breakwater by eigenfunction expansion method, *Ocean Engng*, **23** (1996) 649–666.

9. I. H. Cho and M. H. Kim, Interactions of a horizontal flexible membrane with oblique incident waves, *J. Fluid Mech.* **367** (1998) 139–161.

10. K.-H. Wang and Q. Shen, Wave motion over a group of submerged horizontal plates, *Int. J. Engng Sci.* **37** (1999) 703–715.

11. C. M. Linton and P. McIver, *Handbook of Mathematical Techniques for Wave/Structure Interactions* (Chapman & Hall/CRC, Boca Raton, FL 2001) 304.

12. M. A. Peter, M. H. Meylan, and H. Chung, Wave scattering by a circular elastic plate in water of finite depth: a closed form solution, *IJOPE* **14** (2004) 81–85.
13. A. E. Heins, Water waves over a channel of finite depth with a submerged plane barrier, *Can. J. Math.* **2** (1950) 210–222.
14. C. M. Linton and D. V Evans, Trapped modes above a submerged horizontal plate, *Q. Jl Mech. Appl. Math.* **44** (1991) 487–506.
15. N. J. Balmforth and R. V. Craster, Ocean waves and ice sheets, *J. Fluid Mech.* **395** (1999) 89–124.
16. L. A. Tkacheva, The diffraction of surface waves by a floating elastic plate at oblique incidence, *J. Appl. Math. Mech.* **68** (2004) 425–436.
17. H. Chung and C. Fox, Calculation of wave–ice interaction using the Wiener–Hopf technique, *New Zealand J. Math.* **31** (2002) 1–18.
18. C. M. Linton and H. Chung, Reflection and transmission at the ocean/sea-ice boundary, *Wave Motion* **38** (2003) 43–52.
19. D. V. Evans and M. A. Peter, Reflection of water waves by a submerged horizontal porous plate, *Proceedings of 24th International Workshop on Water Waves and Floating Bodies, Zelenogorsk, Russia* (ed. A. Korobkin & P. Plotnikov; St Petersburg State University, St Petersburg 2009) 82–85.
20. M. H. Meylan, The wave response of ice floes of arbitrary geometry, *J. Geophys. Res.—Oceans* **107**, 2002. Artical No. 3005.
21. T. D. Williams, *Reflections on ice: the scattering of flexural-gravity waves by irregularitiies in Arctic and Antarctic ice sheets*. Ph.D. Thesis, University of Otago, Dunedin, New Zealand (2005).
22. J. B. Lawrie and I. D. Abrahams, An orthogonality relation for a class of problems with high-order boundary conditions; applications in sound-structure interaction, *Q. Jl Mech. Appl. Math.* **52** (1999) 161–181.
23. P. McIver, The dispersion relation and eigenfunction expansions for water waves in a porous structure, *J. Engng Math.* **34** (1998) 319–334.
24. A. Kohout, M. H Meylan, S. Sakai, K. Hanai, P. Leman, and D. Brossard, Linear water wave propagation through multiple floating elastic plates of variable properties, *J. Fluids Struct.* **23** (2007) 649–663.
25. G. Zilman and T. Miloh, Hydroelastic buoyant circular plate in shallow water: a closed form solution, *Appl. Ocean Res.* **22** (2000) 191–198.
26. H. Kagemoto and D. K. P. Yue, Interactions among multiple three-dimensional bodies in water waves: an exact algebraic method, *J. Fluid Mech.* **166** (1986) 189–209.
27. M. A. Peter and M. H. Meylan, Infinite-depth interaction theory for arbitrary floating bodies applied to wave forcing of ice floes, *ibid.* **500** (2004) 145–167.

APPENDIX A

Rigid semi-infinite submerged plate—the dock problem

Here, we give a brief description of the problem of a semi-infinite submerged rigid plate, that is, a submerged dock. The finite and the circular dock can be solved analogously. The solution method presented here is based on that given by (**14**), with some modification. The problem is given by (2.8), (2.9), and (2.10), while (2.11) and (2.12) are replaced by

$$\frac{\partial \phi}{\partial z} = 0, \quad \text{on } z = -d;\ 0 < x < \infty. \tag{A.1}$$

The eigenfunction expansion in the region $x < 0$ is identical to that given by (2.20). In the region $x > 0$, we expand the potential as

$$\phi = \sum_{n=-2}^{\infty} b_n \psi_n(z) \mathrm{e}^{-\kappa_n}, \tag{A.2}$$

where either

$$\psi_n(z) = \begin{cases} \cos(\kappa_n(z+d)), & -d < z < 0, \\ 0, & -h < z < -d, \end{cases} \tag{A.3}$$

or

$$\psi_n(z) = \begin{cases} 0, & -d < z < 0, \\ \cos(\kappa_n(z+h)), & -h < z < -d, \end{cases} \tag{A.4}$$

where κ_n is either the negative imaginary and positive real roots of the dispersion equation $\alpha + \kappa \tan(\kappa d) = 0$ or given by $\kappa_n = n\pi/(h-d)$ for $n = 0, 1, \ldots$ ordered with the imaginary root first and then by increasing size for the positive real roots. We use (A.3) when the κ_n satisfies the dispersion equation and we use (A.4) when κ_n is given by $\kappa_n = n\pi/(h-d)$. The rest of the solution follows exactly as before.

It is noteworthy that the problem of scattering by a semi-infinite submerged dock was solved analytically using the Wiener–Hopf technique a long time ago, compare (**13**). In particular, it was found that the modulus of the reflection coefficient takes a very simple form, namely $|R| = |\kappa - k|/|\kappa + k|$.

APPENDIX B

Orthogonality relation

The eigenfunctions satisfy a special kind of near-orthogonality relation similar to the one found by Lawrie and Abrahams (**22**) for the case of a plate floating on the water surface. We know that

$$\int_{-h}^{0} \partial_z^2 \psi_n \psi_m \, dz = \int_{-h}^{0} \psi_n \partial_z^2 \psi_m \, dz - \partial_z \psi_n(-d)[\psi_m^+ - \psi_m^-] + \partial_z \psi_m(-d)[\psi_n^+ - \psi_n^-] \tag{B.1}$$

which means that

$$\left(\kappa_n^2 - \kappa_m^2\right) \int_{-h}^{0} \psi_n \psi_m \, dz = \frac{\beta}{\alpha} \partial_z \psi_n(-d) \partial_z \psi_m(-d) \left(\kappa_n^4 - \kappa_m^4\right). \tag{B.2}$$

This can be rearranged to give

$$\int_{-h}^{0} \psi_n \psi_m \, dz = \frac{\beta}{\alpha} \partial_z \psi_n(-d) \partial_z \psi_m(-d) \left(\kappa_n^2 + \kappa_m^2\right), \quad m \neq n. \tag{B.3}$$

We will use this in Appendix c.

APPENDIX C

Energy balance

We derive the energy-balance relation for the semi-infinite case for normal incident angle by considering the integral identity

$$\iint_{\mathcal{U}} \left(\phi^* \nabla^2 \phi - \phi \nabla^2 \phi^*\right) dV = \oint_{\partial \mathcal{U}} \left(\phi^* \partial_n \phi - \phi \partial_n \phi^*\right) d\mathcal{S}, \tag{C.1}$$

where ϕ is the solution to (2.8) to (2.12), * denotes conjugation and $\mathcal{U}$ is the region of the plane $-h < z < 0$, $-N < x < N$ with a cut for the submerged plate. Since the Laplacians vanish, we can rewrite this as

$$\operatorname{Im} \oint_{\partial \mathcal{U}} \phi^* \partial_n \phi \, d\mathcal{S} = 0. \tag{C.2}$$

We now evaluate this integral, the contribution from the free surface and from the sea floor is zero so we are left with three integrals to evaluate. Assuming that N is sufficiently large that all the decaying modes can be neglected, we obtain the following contribution from the integral at $x = -N$

$$\operatorname{Im}\left\{\left(\mathrm{e}^{-k_0 N} + a_0^* \mathrm{e}^{k_0 N}\right) k_0 \left(\mathrm{e}^{k_0 N} - a_0 \mathrm{e}^{-k_0 N}\right) \int_{-h}^{0} (\psi_0)^2 \, dz\right\} = \frac{k_0}{\mathrm{i}} \left(1 - |a_0|^2\right). \tag{C.3}$$

The contribution from the integral at $x = N$ is given by

$$\begin{aligned}
&\operatorname{Im}\left\{\int_{-h}^{0} - \left(b_0^* \mathrm{e}^{\kappa_0 N} \psi_0 + b_1^* \mathrm{e}^{\kappa_1 N} \psi_1\right) \left(-\kappa_0 b_0 \mathrm{e}^{-\kappa_0 N} \psi_0 + \kappa_1 b_1 \mathrm{e}^{-\kappa_1 N}\right) \psi_1 \, dz\right\} \\
&= -\frac{\kappa_0}{\mathrm{i}} |b_0|^2 \int_{-h}^{0} \psi_0^2 \, dz - \frac{\kappa_1}{\mathrm{i}} |b_1|^2 \int_{-h}^{0} \psi_1^2 \, dz \\
&\quad - \operatorname{Im}\left\{\kappa_0 b_0^* b_1 \mathrm{e}^{(\kappa_0 - \kappa_1)N} + \kappa_1 b_0 b_1^* \mathrm{e}^{(-\kappa_0 + \kappa_1)N}\right\} \int_{-h}^{0} \psi_0 \psi_1 \, dz.
\end{aligned} \tag{C.4}$$

The contribution from the integral around the plate is given by

$$\operatorname{Im} \int_0^N [\phi^- - \phi^+]^* \partial_z \phi \, dx = \operatorname{Im} \int_0^N \frac{\beta}{\alpha} \partial_x^4 \partial_z \phi^* \phi_n \, dx \tag{C.5}$$

and using integration by parts, we obtain

$$\operatorname{Im} \int_0^N \frac{\beta}{\alpha} \partial_x^4 \phi^* \partial_z \phi_n \, dx = \operatorname{Im}\left\{ \frac{\beta}{\alpha} \partial_x^3 \phi_n^* \phi_n \Big|_{x=N} - \frac{\beta}{\alpha} \partial_x^2 \phi_n^* \partial_x \phi_n \Big|_{x=N} \right\} \tag{C.6}$$

$$\begin{aligned}
&= \operatorname{Im}\left\{\frac{\beta}{\alpha}\left(\kappa_0^3 b_0^* \partial_z \psi_0(-d) \mathrm{e}^{\kappa_0 N} + \kappa_1^3 b_1^* \partial_z \psi_1(-d) \mathrm{e}^{\kappa_1 N}\right)\left(b_0 \partial_z \psi_0(-d) \mathrm{e}^{-\kappa_0 N} + b_1 \partial_z \psi_1(-d) \mathrm{e}^{-\kappa_1 N}\right)\right. \\
&\quad \left. + \left(\kappa_0^2 b_0^* \partial_z \psi_0(-d) \mathrm{e}^{\kappa_0 N} + \kappa_1^2 b_1^* \partial_z \psi_1(-d) \mathrm{e}^{\kappa_1 N}\right)\left(\kappa_0 b_0 \partial_z \psi_0(-d) \mathrm{e}^{-\kappa_0 N} + \kappa_1 b_1 \partial_z \psi_1(-d) \mathrm{e}^{-\kappa_1 N}\right)\right\}
\end{aligned} \tag{C.7}$$

$$\begin{aligned}
&= 2\frac{\beta}{\alpha} \frac{\kappa_0^3}{\mathrm{i}} \partial_z \psi_0(-d)^2 |b_0|^2 + 2\frac{\beta}{\alpha} \frac{\kappa_1^3}{\mathrm{i}} \partial_z \psi_1(-d)^2 |b_1|^2 \\
&\quad + \operatorname{Im} \frac{\beta}{\alpha} \left(\left(\kappa_0^3 + \kappa_0^2 \kappa_1\right) b_0^* b_1 \mathrm{e}^{(\kappa_0 - \kappa_1)N} + \left(\kappa_1^3 + \kappa_1^2 \kappa_0\right) b_1^* b_0 \mathrm{e}^{(\kappa_1 - \kappa_0)N}\right) \partial_z \psi_0(-d) \partial_z \psi_1(-d).
\end{aligned} \tag{C.8}$$

We use the identity given by (B.3),

$$\int_{-h}^{0} \psi_0 \psi_1 \, dz = \frac{\beta}{\alpha} (\kappa_0^2 + \kappa_1^2) \partial_z \psi_0(-d) \partial_z \psi_1(-d), \tag{C.9}$$

and observe that (because κ_0 and κ_1 are purely imaginary) all contributions with terms involving both b_0 and b_1 vanish. We are left with the equation

$$k_0|a_0|^2 + \kappa_0|b_0|^2 \int_{-h}^{0} \psi_0^2\, dz + \kappa_1|b_1|^2 \int_{-h}^{0} \psi_1^2\, dz$$

$$-2\frac{\beta}{\alpha}\kappa_0^3 \partial_z \psi_0(-d)^2|b_0|^2 - 2\frac{\beta}{\alpha}\kappa_1^3 \partial_z \psi_1(-d)^2|b_1|^2 = k_0, \tag{C.10}$$

which represents energy balance.